An Experimental Study for Noise Reduction of the Cross-Flow Fan of the Room Air-Conditioners

Hyoung Mo Koo*

Key words : Cross-flow fan, Source spectral distribution function, Velocity auto-spectrum, Noise reduction

Abstract

Present study explains some experimental results on the aerodynamic noise of the cross-flow fan usually installed in the indoor unit of the room air-conditioners and provides a simple reduction method of radiating sound to decrease the total noise level. The spectra of the noise of the cross-flow fan were analyzed by the spectral decomposition method to characterize the generated sound. The unsteady fluctuating flow field was also measured using the I-type hot-wire probe. Comparing the spectral characteristics of the sound and the flow velocity, a useful noise reduction method was proposed, which bounds the region with a fence where the flow fluctuations were noticeably changed in the same fashion as the source spectral distribution functions vary. To validate the proposed method for reducing noise generated by the cross-flow fan, the sound pressure levels of the cross-flow fan system were compared with and without the bounding fence for various flow rates.

Nomenclature

a : sound speed [340 m/s]

BPF : Blade Passing Frequency [Hz]
BPF=NZ

* Development Group, Refrig. & Air-Conditioner Division, Samsung Electronics, Co., LTD. 416, Maetan-3Dong, Paldal-Gu, Suwon City, Kyungki-Do, Korea

Q : flow rate [m^3/sec]

Δp_t : fan total pressure rise [Pa]

D : fan diameter [m]

f : frequency [Hz]

Δf_{ref} : frequency resolution [Hz]

$F^2(St, \phi)$: source distribution function

$G^2(He, \phi, x/D)$: system frequency response function

$G_{vv}(f)$: velocity magnitude auto-spectrum

He : Helmholtz number, $He=\frac{fD}{a}$

L_{pp} : sound pressure level spectral density

N, n : fan rotational speed [rpm, or rps]

P_{ref} : acoustic reference pressure [20 μPa]

S_{pp} : acoustic pressure auto-spectral density

St : Strouhal number,

$$St=\frac{fD}{V_{tip}}\frac{\pi}{Z}=\frac{f}{BPF}$$

x/D : measurement location

V_{tip} : fan tip speed [m/s]

Z : number of fan blade

W : width of heat exchanger [m]

u : velocity [m/s]

Greek symbols

ϕ : flow coefficient

ψ : total pressure coefficient

η : efficiency

ρ : air density

1. Introduction

With increasing customer's expectation of lower noisy operation of the electric home appliance devices, much effort has been drawn into developing the noise reduction methods in this field. The roon air-conditioner is one of the main noisy household electric devices and to reduce the noise level had become the main topic of the developing stage. Among the main components of the air-conditioning system, the fan-duct system is often regarded as the dominant noise source. The typical indoor units of the split type air-conditioners generally take the cross-flow fans as the main air-moving component to circulate the room air through the unit. The cross-flow fan generally incorporates a scroll casing and a stabilizer to form the air-moving system. The former converts the dynamic head of the air into static pressure rise and the latter stabilizes the eccentric vortex flow of a cross-flow fan. A schematic diagram of the indoor unit and the internal streamlines is shown in Fig.1.

The sound generated by the cross-flow fan has large portion of the acoustic power mostly distributed over lower frequency region around the Blade Passing Frequency(BPF) and 30~80% of the BPF regardless of the fan performance and efficiency, which prohibits the fan from being applied to the cases of high pressure rise and rotational speed[1]. However, any approach has yet not been attempted to investigate this type of noise characteristics.

The noise reduction effort of the cross-flow fans hitherto has been carried out in two different ways. The first is to diminish the discrete tonal noise of the BPF and its harmonics. These approaches make use of the cross-flow

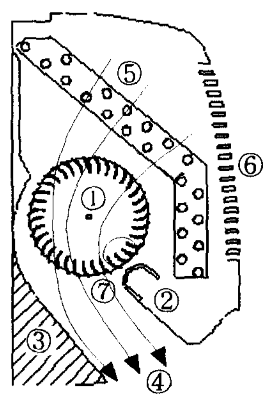

① cross-flow fan ⑤ heat exchanger

② stabilizer ⑥ inlet grill

③ scroll ⑦ fan-stabilizer gap (ε)

④ flow exit

Fig. 1 Schematic view of air-conditioner indoor unit.

fans with randomly distributed blades[2], with skewed blades along the fan span[3], or with skewed stabilizers[4,5]. They generally depend on discrete or continuous modulation technique in frequency domain, which distribute acoustic energy at the BPF and its harmonics over some frequency range centered at those frequencies. Even though these methods have proved to be very effective in reducing discrete tones, overall noise levels can not be lowered because the tonal acoustic energy remains unchanged. The other way is to improve the aerodynamic efficiency of the fan system by optimizing the fan and its component geometry, which thus results in reduced specific noise level. Several parametric studies were carried out on the design values and factors of the fan blades[6], the shapes of the stabilizers[7], and the diffusive profiles of the scrolls[8]. While the results of these types of approach have been very helpful to the engineers in the design stages, spectral characteristics of the generated sound are generally not explained so that the noise reduction efforts can not proceed any further after the parametric optimization has been completed.

This study is composed of several parts. The noise spectra of the cross-flow fans are measured at several operating points on the performance curve. These spectra are analyzed by the spectral decomposition method to eliminate any influence of the radiation characteristics of the duct or the experimental rig. And the fluctuating velocity spectra are also measured using the hot wire probe at several locations around the fan's inlet and outlet regions with varying the fan loading. The possible main noise source region of the cross-flow fan system is conjectured by comparing the sound and velocity spectra. Finally some modifications are tried on the boundary geometry to block the flow region to which the fan noise is closely related. Finally the resulting noise characteristics are explained.

2. Experimental apparatus

The fan testing system used to measure the performance characteristics of the cross-flow fan system was based on ASHRAE standard 51-1985(Laboratory Methods of Testing Fans for Rating). An experimental rig is connected to the right end of the fan tester that represents the indoor unit. Several screens are installed upstream of the fan to simulate the flow resistance of the heat exchanger(Fig. 2). The cross-flow fan used in this study has the following specifications.

Impeller diameter: 95mm
Blade chord length: 13mm
Blade span: 70mm
Number of span-wise subsections: 4
Number of blades: 35

The mean chord of the blade cross section is of circular arc profile and is set by 27°

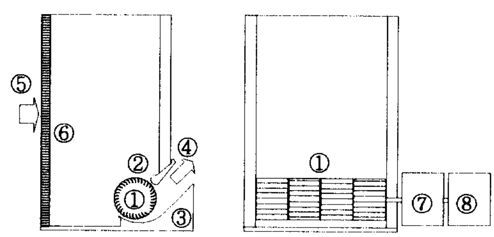

① cross-flow fan ⑤ flow from the fan tester
② stabilizer ⑥ screen
③ casing ⑦ torque meter
④ flow exit ⑧ servo-motor

Fig. 2 The experimental rig to simulate the indoor unit.

with respect to the fan radial line. Fan torque was measured by the torque meter (ONOSOKI, 5 Kg_f-cm) which is serially connected by two coupling to the rotating shaft and to a servo-motor (TOEI, 0.4kW, 4000rpm) to drive the fan. This torque value was used to calculate the aerodynamic efficiency of the fan with the flow rate and the pressure rise measured by the fan tester.

All of the flow quantities measured are expressed using the following non-dimensional terms.

$$\phi = \frac{Q}{\pi N D^2 L} \tag{1}$$

$$\psi = \frac{\Delta P_t}{\rho N^2 D^2/2} \tag{2}$$

$$\eta = \frac{Q \cdot \Delta P_t}{2\pi T N} \tag{3}$$

Here, Q and ΔP_t are the flow rate (m^3/sec) and the total pressure rise (Pascal) of the fan, respectively. L and D are the span-wise length and diameter of the cross-flow fan, and ρ is the air density. Also T and N are input torque (N-m) to the fan and the rotational speed(rps).

The noise levels of the cross-flow fan system were measured in an anechoic chamber, which is 5m×5m×3m, with ambient noise and cut-off frequency of 15dB and 125Hz, respectively. The upstream screens of the experimental rig were used to impose flow resistance (i.e., pressure loss) on the fan. The sound pressure signal measured by the microphone was analyzed using a B&K 2032 waveform analyzer to calculate the sound spectra. Two hundred averages were performed with 50% overlap. The microphone is located 0.5m downstream of the flow exit and the predetermined resistance is connected to the fan apparatus.

3. Noise characteristics of the cross-flow fans

To investigate the noise generation by the cross-flow fan, it is indispensable to make use of the spectral characteristics of the sound. The spectral characteristics might be influenced by the acoustic trend of flow conditions and the propagation path, and consequently be changed in shapes and magnitude. It is even more difficult to discriminate the differences among sound spectra for various operating conditions. It is thus necessary to eliminate these acoustic effects of the surroundings and flow rates in order to compare the spectra at different operating points and specify the noise characteristics. This paper followed the spectral decomposition procedure for obtaining the spectral characteristics of the sound generated by the cross-flow fan only.

3.1 Spectral decomposition method

Present study made use of the simplified experimental rig to simulate the flow field of the cross-flow fan in the air-conditioners. In order to investigate the noise generated by the cross-flow fan only, it is necessary to eliminate any acoustic effect of experimental rig in real device geometry. The spectral decomposition method was used to identify the noise characteristics of the cross-flow fan. This method is principally based on the acoustic similarity laws of Weideman[9] for non-dimensional fan noise spectra and was extended by Mongeau [10,11] to be applicable to both ducted and unducted turbomachinery. With this approach, it was possible to filter out any common acoustic trend of the noise spectra at different rotational speed and characterize both the acoustic response effects and the aerodynamic sound generating phenomena. The resulting sound spectra for various operating conditions were compared to specify the differences of the generating mechanism. The decomposition procedures used in this study are briefly summarized as follows.

The sound pressure level spectral density, L_{pp} is defined by the following equation,

$$L_{pp} = 10 \log [S_{pp} \triangle f_{ref} / p_{ref}^2] \tag{4}$$

Here the acoustic pressure auto-spectral density, S_{pp}, is scaled as following form,

$$S_{pp}(f, V_{tip}, \phi, x) \sim [\rho_o \cdot V_{tip}^2]^2 \cdot (D/V_{tip}) \tag{5}$$

S_{pp} can be expressed by the product of two non-dimensional functions,

$$\frac{S_{pp}(f, V_{tip}, \phi, x)}{[\rho_o \cdot V_{tip}^2]^2 (D/V_{tip})} = G^2(He, \phi, x/D) \cdot F^2(St, \phi) \tag{6}$$

Equation(6) is substituted to obtain the following expression, which can be used to get the relationship between the sound pressure level and the non-dimensional function

$$20 \log G(He) = L_{pp}(f, V_{tip}) - 30 \log V_{tip} - 10 \log \frac{\rho_o^2 D \Delta f_{ref}}{p_{ref}^2} - 20 \log F(St) \tag{7}$$

where the flow rate and the x/D remain constant and p_{ref} is 20μPa. The 20logG(He) is the system frequency response function, which describes any sound propagation effect between the source and the microphone. The 20logF(St) is called the source spectral distribution function(SSDF), representing the aerodynamic sound generation related to the flow fluctuations inside the cross-flow fan and the near field acoustic interactions. The equation (7) is used to remove G-term from the normalized spectra in order to obtain the desired information on the sound source characteristics. The SSDF can be obtained from the above equation using the L_{pp}'s for several rotation speeds. More details about the procedure are out of scope of this paper and can be found in ref.[11].

3.2 Spectral characteristics of the sound generated by the cross-flow fan

Figure 3 is the performance characteristics of the cross-flow fan used in this study. This performance curve shows general features of the cross-flow fan characteristics.

Several points on the performance curve were

Table 1 Specification of the load conditions

	ⓐ	ⓑ	ⓒ	ⓓ	ⓔ
ϕ	0.724	0.650	0.584	0.517	0.471
η (%)	13.8	21.7	27.6	34.4	36.7

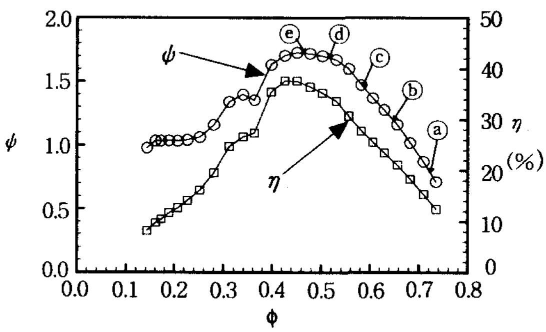

Fig. 3 The non-dimensional performance curve of the cross-flow fan used in this study.

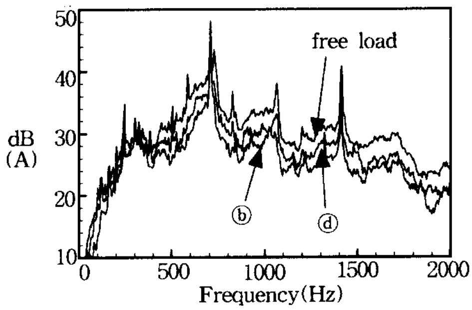

Fig. 4 The comparison of the A-weighted sound spectrums of the cross-flow fan at various operating points at 1210 rpm.

selected to measure the sound spectral characteristics of the fan. The values of the flow coefficients and the efficiency of each point are represented in Table 1 and are indicated in Fig. 3. With the fan rotational speed of 1210 rpm, the values of accompanying overall sound pressure levels are 56.9, 55.7, 55.9, 53.5, and 52.0 dB(A) respectively. Since this study was mostly interested in the stably operating region, only the righthand side of the maximum pressure point on the performance curve was chosen where the head rise coefficient is continuously decreasing with increasing flow rate. Particularly, the operating points used in the air-conditioners are generally located in the range between ⓑ and ⓓ. The spectra at three different operating conditions, free load, ⓑ and ⓓ of Fig. 4, where the free load condition means operation without any flow resistance and indicates the rightmost point on the performance curve with zero static pressure rise. The sound spectra were obtained after 200 averaging processes with a 50% overlaps and the band width was 4Hz. Any clear difference cannot be discerned among the acoustic signatures only except that the overall sound pressure levels are diminishing as the flow rates are decreased or the efficiency is increased. This is the reason that the acoustic decomposition method should be used in this study to discriminate the sound generation characteristics of the cross-flow fan from other radiation influences under various operating conditions.

To get the SSDF at various load conditions of Fig. 3, total eight frequency spectra were used at each point which were measured in the range of 1105~1350rpm, which was stepped by 35 rpm. The several source spectral distribution functions are represented in Fig. 5. Each plot consists of four source spectra for clear presentation, each measured at a different rotational speed, 1175, 1210, 1245, 1280 rpm, respectively. Some scatters shown in the plots were supposed to be due to the numerical truncation errors and the intrinsic nature of the free field measurements (see Fig. 9 of [11]), where the latter was inevitable in the present experiments considering measurement location.

In the high flow rate region, the source spectral distribution are typically dominated by pure tones at the BPF and its first harmonic (St=1,2), and other small tones are also present at multiples of the shaft speed frequency (see Fig. 6 of [13]). These nearly discrete frequency phenomena stem from the interaction of the rotating spatially non-uniform mean flow at the impeller discharge with the stationary cut-off and other duct components, and become lowered in magnitude as the flow rate is diminished. The related unsteady flow structure is still unknown and out of scope of this study.

These plots show two distinctive natures of the sound characteristics of the cross-flow fan. The first is that the levels of the higher frequency components (1<St) are decreasing as the flow rate is lowered, which means that the absolute velocity around the fan blades is reduced, consequently actual magnitude of the

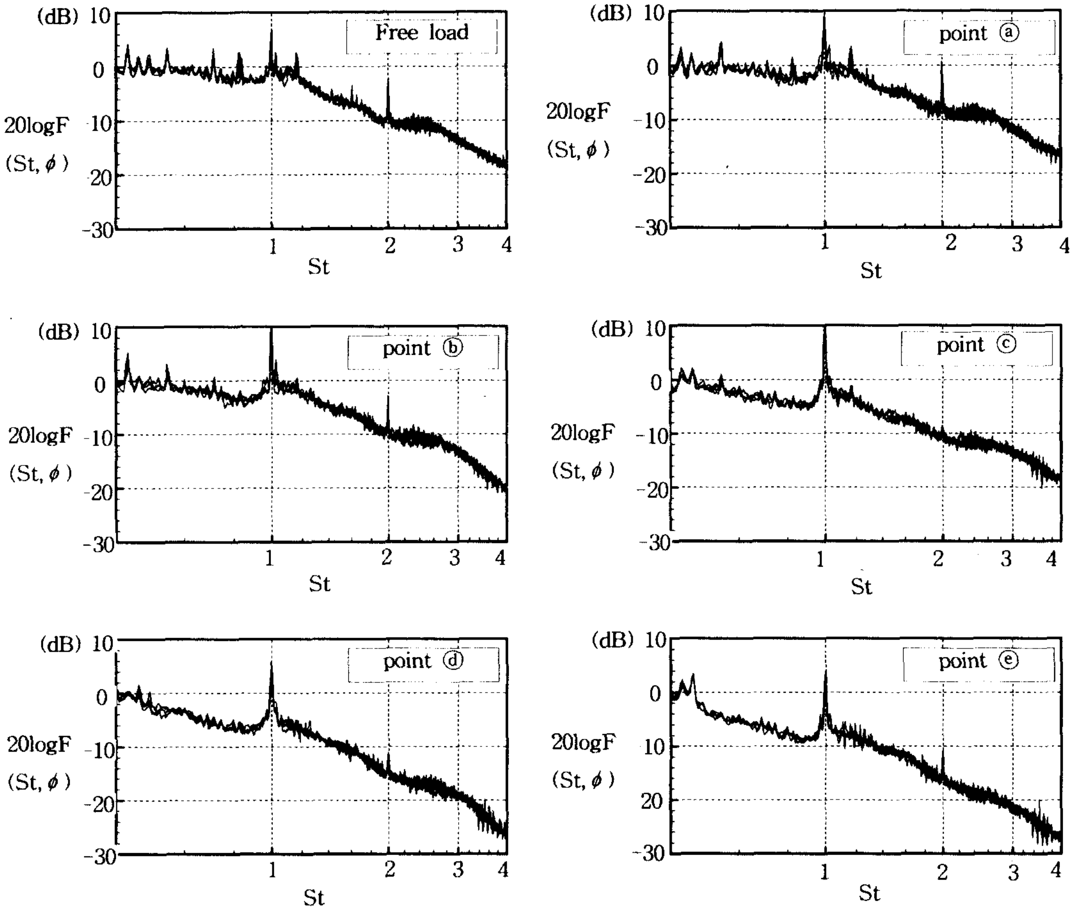

Fig. 5 The source spectral distribution functions of the sound generated by the cross-flow fan at various operating points of Fig. 3.

flow fluctuations becomes smaller. The spectra of these components are decreased in parallel way in that the slope of the plots are maintained nearly unchanged as the flow rate varies. The other characteristics is that the shapes of the SSDF's vary over the frequency region where the value of St is less than or around 1. The acoustic power in that region is remarkably reduced as the flow rate is decreased or the aerodynamic efficiency of the fan is increased. More specifically, the values of the source spectral distribution functions around St=1 become remarkably reduced as the flow rate decreases. Considering the logarithmic scale of the source functions, this phenomenon is regarded as the main reason of the reduced overall pressure levels with decreasing flow rate.

3.3 Fluctuating characteristics of the flow field around the cross-flow fan.

The flow sound of the turbomachinery is generally originated from the unsteady fluctu-

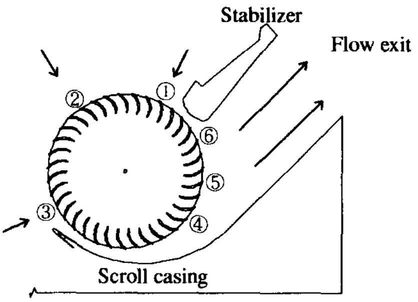

Fig. 6 The measurement locations of the hot wire probe for the fluctuating velocity magnitude spectrums.

ating flow field around the impellers and its interaction with other components of the accompanying ducts. The cross-flow fan considered in this study has several parts to compose the air-moving system. This means that there are various sound sources to be considered. Also the non-uniform flow field around the fan can be another source of pressure fluctuations on the fan blades. To investigate the relationship between the generated sound and the fluctuating flow field, the approach adopted in the present study is to measure the auto-spectral density functions, $G_{vv}(f)$ of the flow velocity around the fan at various operating conditions of Fig. 3. Total six points were selected around the cross-flow fan, three points are located in the flow inlet region and the others in the flow discharge region (see Fig. 6). Considering the blade pitch angle ($360^\circ/35 \fallingdotseq 10.3^\circ$) and the number of the blades between neighboring measurement points, exact locations can be calculated from Fig. 6. One single-wire probe manufactured by KANOMAX was used with 5 μm Walleston wire and anemometer electronics. The hot-wire was positioned 2mm away radially from the blade tips. The velocity magnitude data near the blade leading and the trailing edges have strong periodicity at the fan blade rate. This was determined from the

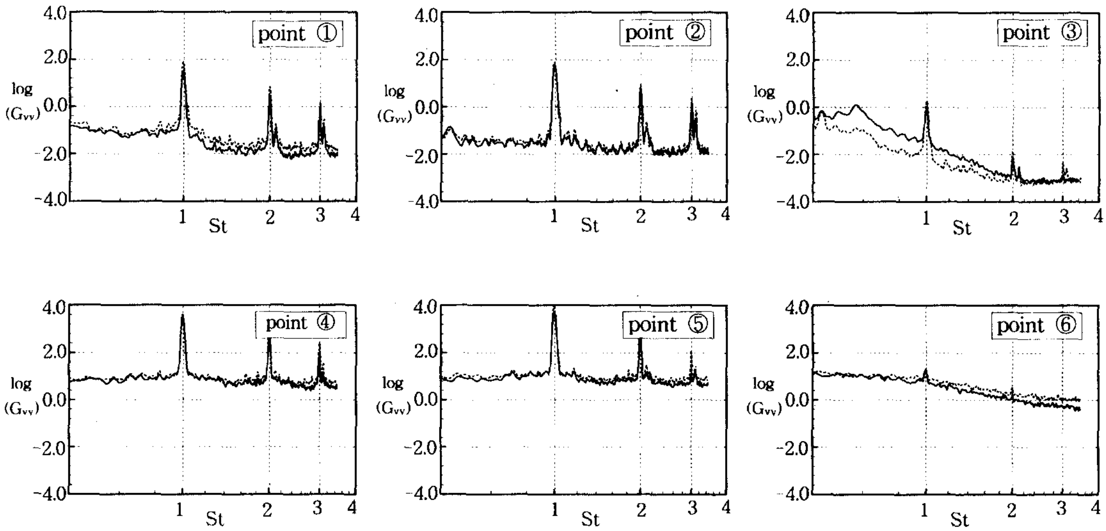

Fig. 7 The velocity magnitude auto-spectra at various locations around the cross-flow fan shown in Fig. 6; dashed line, operating point ⓑ; solid line, operating point ⓓ of Fig. 3.

measured hot-wire signal by using a synchronous phase averaging technique. All hot-wire data were sampled in conjunction with a signal from a hole sensor located at the casing surface, which sensed the passing of the magnet attached to the rim of the fan, producing a 5 volt pulse once per revolution of the fan.

In Fig. 7 are represented the auto-spectra of the velocity magnitude measured at several points around the fan in Fig. 6, where the comparison can be made between two operating conditions, ⓑ and ⓓ of Fig. 3. All of the velocity spectra were made non-dimensional by the blade tip speed(V_{tip}) for comparison and the abscissa is represented by the logarithmic values of the St number in order to be compared to the shapes of the SSDF's of the sound in the previous section. As usually expected, the BPF and its harmonic components are dominant in the auto-spectra regardless of the measurement locations except ⑥. The spectral signature at ⑥ is a little surprising in that the BPF tone has been known to be originated from the interaction between rotating flow field and the stationary stabilizer. Even considering the flow streamline depicted in Fig. 1 around the stabilizer, where the hot-wire probe at ⓑ is included in the recirculating region with relatively low mean flow velocity, this spectrum was unexpected and it was concluded that this region has not well defined periodic flow structure responsible for the discrete tones. Comparatively, the shapes of the auto-spectra in the flow region, ①~③, are noticeably changed according to the measurement locations. This means that the inlet flow

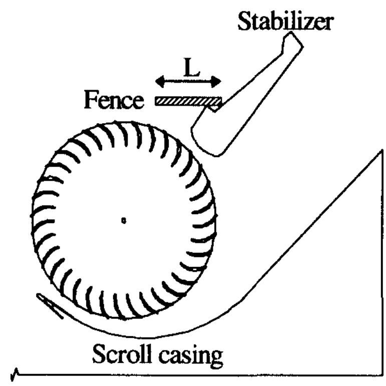

Fig. 8 The fence bounding the flow fluctuating region to reduce the noise generation (L denotes the fence length).

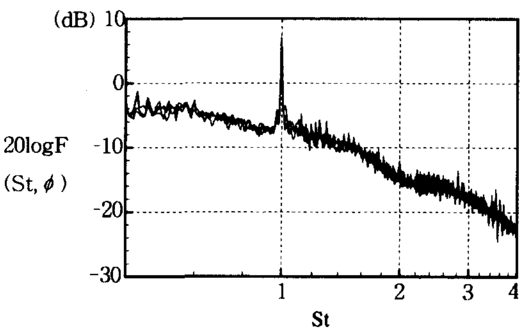

(a) ϕ = 0.593 (η = 25.8%)

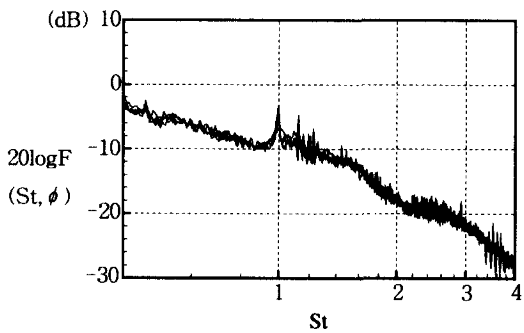

(b) ϕ = 0.482 (η = 36.5%)

Fig. 9 The source spectral distribution functions at two different operating conditions with the fence of L=30 mm of Fig. 8.

conditions are not uniform on the fan's periphery and the blade loading is continuously changing as the fan blades rotate in the inlet region. Considering the difference of the loading conditions, both ends of the inlet, ① and ③, have opposite trend of the spectra. The spectral power of the fluctuating velocity is highest in the region, ①, where, after passing the stabilizer surface, the fan blade firstly meets incoming air flow and the flow angle is significantly changed as the blades rotate. The exact flow field in this region is very complex and unstable, which requires future study.

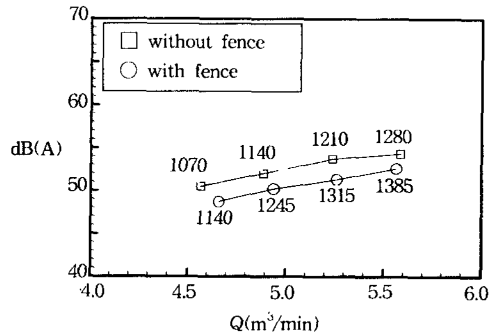

Fig. 10 The sound pressure levels of the cross-flow fan (L=30mm).

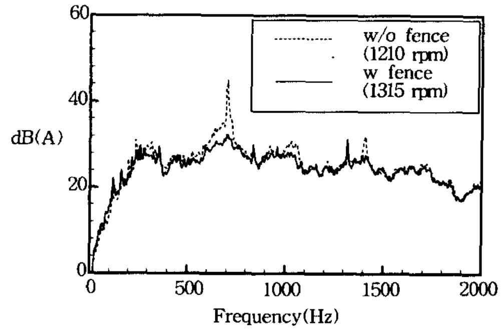

Fig. 11 The comparison of the noise spectrums of the cross-flow fan of the Fig. 10 (L =30mm).

4. Noise reduction of the cross-flow fans

Comparing the SSDF's of Fig. 5 and the auto-spectra of Fig. 7, spectral signatures of the aerodynamic noise of the cross-flow fan can be related to the fluctuating flow field around the fan. Considering the source spectral distribution functions of various operating conditions, two main variations of the noise characteristics can be found. The first is that the lowered flow rate results in the reduced sound pressure levels of the higher frequency components. Also the lower flow rate or the increased efficiency gives rise to even more remarkable reduction in the low frequency region as previously mentioned. Scrutinizing the velocity auto-spectra in the previous section, similar trends can be found in the region ①, just upstream of the stabilizer. With this comparison, present study assumed that the region ① is most closely related to the noise generation of the cross-flow fan.

To reduce the velocity fluctuations in the region, a fence of length, L was installed in the just upstream region of the stabilizer as depicted in Fig. 8.

The remaining paragraphs explain the experimental results concerning the fence of length, L=30mm, which was very effective in reducing the noise level and whose performance variation was relatively acceptable in that the proper increment of the rotational speed (here, 105rpm) could compensate the accompanying drop of fan's pumping capacity.

In Fig. 9 are represented the source spectral distribution functions of two different operating conditions with the bounding fence. Comparing these two plots with the corresponding ⓒ and ⓔ of Fig. 5 shows that the SSDF decreases by considerable level, indicating the reduced sound power. Though not shown in the plots, the SSDF levels in the low frequency region ($St<0.4$) are diminished by nearly same level.

By fixing the flow resistance and varying the rotational speed of the fan, the relationship between flow rate and the noise levels could be obtained. The resistance passing through the point ⓓ of Fig. 3 was chosen to represent that of the typical heat exchanger of the air-conditioners. With this resistance, noise levels of the cross-flow fan versus flow rate were measured and represented in Fig. 10 for different rotational speeds in the parenthesis on the plots. The A-weighted overall sound pressure levels were reduced by nearly 2~3dB(A) with the fence over the entire experimental range. To compare the spectral characteristics of the noise, frequency spectra at nearly same flow rates were represented in Fig. 11. Comparing these two sound spectra, the difference between two spectra can hardly be discerned in the high frequency region. The main noise reduction effect stems from the lower frequency components of the spectra where the value of St is less than or around 1. Considering both the sound pressure levels with flow rates and the shape change of the sound spectra, it is inferred that the noise reduction effect using the bounding fence in this region is not due to the decreased flow rate or pumping capacity but stems from the suppression of low frequency fluctuations around the fan blades.

5. Conclusion

In this study the sound generation of the cross-flow fan of the indoor unit of the room air-conditioners was investigated. The acoustic signatures for various operating conditions have been analyzed using the spectral decomposition method based on the acoustic similarity of the turbomachinery. The source spectral distribution functions significantly varied in level and shape with the loading conditions. The velocity auto-spectra were also measured using the I-type probe at several locations around the cross-flow fan. Comparing the variation of the acoustic signatures and that of the velocity auto-spectra for different operating conditions, the just upstream region of the stabilizer was supposed to be the dominant sound generating region and to be closely related to the lower frequency noise components. Considering the above result, a simple noise reduction method was proposed, which installs a bounding fence around this region. The sound pressure levels of the cross-flow fan system were considerably reduced with the present method, where particularly the acoustic power in the lower frequency region (where the Strouhal number is lower than or around 1) was diminished under the typical resistance condition of the air-conditioner heat exchanger. Considering the variation of the sound spectra, it is inferred that the reduction effect using the bounding fence in this region stems from the suppression of low frequency fluctuations around the fan blades.

References

(1) Ikui Takefumi and Inoue Masahiro, 1988, Turbo-blowers and compressors. Corona Publishing Co., Tokyo Japan, pp. 297-304.

(2) Hayashi, T., Kobayashi, Y., Nagamori, A., and Horino, H., 1996, Low-noise design for cross-flow fans based on frequency modulation, Trans. Jpn. soc. mech. Eng. (C), Vol. 62, No. 601, pp. 68-73.

(3) Hayashi, T., Kobayashi, Y., Nagamori, A., and Horino, H., 1998, Low-Noise Design for Cross-Flow Fans (Reduction of Blade

Passing Tones by Noise Source Interference), Trans. Jpn. soc. mech. Eng. (C), Vol. 64, No. 617, pp. 218-223.
(4) Lee, D. S., Jeng, M. S., and Tsau, F., 1997, Noise reduction of a cross flow fan, Proceedings, inter-noise 97, pp. 403-406.
(5) Koo, H. M., Lee, J. K., Kim, C. H., and You, K. C., 1998, A study on the noise reduction of a cross-flow fan of the air-conditioners using the skewed stabilizers, Proceedings, inter-noise 98, Christchurch, New-Zealand.
(6) Fukano, T., 1992, A study on the noise reduction of the cross-flow fans (1st report; The effects of the rotor blades and the stabilizers), Turbomachinery journal, Vol. 20, No. 8, pp. 22-28.
(7) Fukano, T., 1993, A study on the noise reduction of the cross-flow fans (2nd report; The effects of the profiles of the stabilizers), Turbomachinery journal, Vol. 21, No. 6, pp. 30-35.
(8) Fukano, T., 1993, A study on the noise reduction of the cross-flow fans (3rd report; The effects of the profiles of the scrolls), Turbomachinery journal, Vol. 21, No. 8, pp. 16-22.
(9) Weidemann, J., 1971, Analysis of the relations between acoustic and aerodynamic parameters for a series of dimensionally similar centrifugal fan rotors, NASA technical translation TT F-13, 798.
(10) Mongeau, L., 1991, Experimental study of the mechanism of sound generation by rotating stall in centrifugal turbomachines, Ph.D. Thesis, The Pennsylvania State University, PN, U.S.A.
(11) Mongeau, L., Thompson, D. E., and McLaughlin, D. K., 1995, A method for characterizing aerodynamic sound sources in turbomachines, Journal of sound and vibration, Vol. 181, No. 3, pp. 369-389.
(12) Bent, P. H., and McLaughlin, D. K., 1993, Enhancements to noise sources measurement techniques for turbomachinery, AIAA paper 93-4373.
(13) Mongeau, L., Thompson, D. E., and McLaughlin, D. K., 1993, Sound generation by rotating stall in centrifugal turbo machines, Journal of sound and vibration, Vol. 163, No. 1, pp. 1-30.